© 2015. Published by The Company of Biologists Ltd | Journal of Cell Science (2015) 128, 3837 doi:10.1242/jcs.180463

CORRECTION

Characterization of Cep85 – a new antagonist of Nek2A that is involved in the regulation of centrosome disjunction

Canhe Chen, Fang Tian, Lin Lu, Yun Wang, Zhe Xiao, Chengtao Yu and Xianwen Yu

There was an error published in *J. Cell Sci.* **128**, 3290-3303.

In the Materials and Methods under 'siRNA', the incorrect sequence for Cep85 was given. The correct sequence is given in the section below.

siRNA

RNA oligonucleotide duplexes were synthesized by Shanghai GenePharma (Shanghai, China) and the sequences were as follows: Cep85, 5′-GGAGA-CACUUUAUUCAGAUtt-3′; Nek2A, 5′-AAACAUCGUUCGUUACUAUtt-3′; and negative control siRNA, 5′-UUCUCCGAACGUGUCACGUtt-3′. All siRNAs were transfected using ribo*FECT* CP (RiboBio, Guangzhou, China) and cells were analyzed 72 h after transfection.

The authors apologise to the readers for any confusion that this error might have caused.

Journal of Cell Science (2015) 128, 3290-3303 doi:10.1242/jcs.171637

Fig. 6. Depletion of Cep85 results in centrosome splitting, similar to the effect of Nek2A overexpression, and disappearance of the rootletin signal at centrosomes in G2. (A) Schematic outline of experiments shown in B–E. HeLa cells were transfected with siRNA followed by a double thymidine block and release at G2 phase prior to analysis. (B) Cells were fixed and immunostained with antibodies against Cep85 (green) and γ-tubulin (red). (C) The efficiency of siRNA to deplete endogenous Cep85 is shown by western blotting (IB). (D) The histogram indicates the distance between centrosomes. ***P*<0.01. (E) The histogram indicates the percentage of cells with separated centrosomes. A centrosome distance exceeding 2 µm was counted as separated. ****P*<0.001. (F) Schematic outline of experiments shown in G–J. HeLa cells were subjected to a double thymidine block and release to enrich them at G1/S. HA–Nek2A was transfected into the cells at the indicated time point, 20 h prior to analysis. (G) Cells were fixed and subjected to immunostaining with antibodies to stain HA–Nek2A (red) and γ-tubulin (green). (H) The expression levels of HA–Nek2A in cells are shown by western blotting. (I) The histogram indicates the distance between centrosomes. ***P*<0.01. (J) The histogram indicates the percentage of cells with separated centrosomes. Centrosome distance exceeding 2 µm was counted as separated. ****P*<0.001. (K) Immunofluorescence analysis of rootletin in Cep85-depleted cells. U2OS cells were treated according to the procedure shown in A. Cells were fixed and immunostained with antibodies against Cep85 (red), γ-tubulin (green) and rootletin (purple). (L) The histogram indicates the percentage of cells lacking rootletin signal at centrosomes in G2 after Cep85 depletion. ****P*<0.001. In B, G and K, the enlarged view of the boxed area is shown in the inset on individual image, and the magnified view of the boxed centrosome in the merged image is illustrated on the right. Scale bars: 5 µm. In D, E, I, J and L, results are from three independent experiments with 30 cells were analyzed for each experiment; data are mean±s.e.m. NSC, non specific control siRNA.

Given that upregulation of Cep85 can inhibit Nek2A activity, we reasoned that reducing Cep85 protein levels would lead to an enhancement of the activity of Nek2 and premature centrosome separation. We found that is indeed the case as ∼40% of those cells with no detectable level of Cep85, which was depleted by siRNA, displayed premature separation of centrosomes (Fig. 6B–E). This

Journal of Cell Science (2015) 128, 3290-3303 doi:10.1242/jcs.171637

was very similar to the effect of Nek2A overexpression that caused splitting of centrosomes in ∼50% of cells (Fig. 6F–J). We also observed that over 80% of cells with non-detectable level of Cep85 completely lost rootletin at centrosomes in G2/M phase (Fig. 6K,L). Thus Cep85 might play some roles that are opposite to Nek2A in maintenance of centrosome integrity in the S and G2 phases. However, this might simply occur through altering the centrosome structure or accumulation of Nek2A at centrosomes. To rule out these possibilities, we examined the localization and intensity of γ-tubulin and Nek2A after both up- or down-regulation of Cep85. We found that neither up- nor down-regulation of Cep85 changed the intensity or centrosome localization of γ-tubulin and Nek2A, although centrosome splitting revealed by staining either Nek2A or γ-tubulin was easily detected in those Cep85-depleted cells (supplementary material Fig. S4). Thus, both experiments with up- and down-regulation of Cep85 expression indicate that Cep85 antagonizes Nek2A activity in cells.

Cep85 inhibits Nek2A kinase activity, and the Cep85 region containing amino acids 257–433 is sufficient to bind to and inhibit Nek2A *in vitro*

Given that Cep85 can negatively regulate Nek2A activity in cells, we thus sought to determine the mechanism by which Cep85 could suppress Nek2A activity. We first examined whether Cep85 could inhibit Nek2A kinase activity. Nek2 kinase activity can be measured by an *in vitro* kinase assay with β-casein as a substrate (Fry et al., 1995). We found that GST–Cep85 could efficiently suppress Nek2A kinase activity in a dosage-dependent manner and that GST–Cep85 itself was not phosphorylated by Nek2A (Fig. 7B), suggesting that Cep85 is not be a substrate for Nek2A. We next determined which region in Cep85 was responsible for the inhibition of Nek2 kinase activity. A series of Cep85 truncated mutants were expressed and purified as GST fusion proteins (Fig. 7A), and Nek2A kinase activity was assessed in the presence of various Cep85 proteins. We found that those mutants harboring amino acids 257–433, including M12, M13, M14 and M15, retained full inhibitory activity towards Nek2A, similar to WT (Fig. 7A,C). Those mutants containing regions outside of amino acids 257–433, including M1, M17 and M9, failed to inhibit Nek2A; two additional mutants M11 (amino acids 1–349) and M16 (amino acids 350–762) containing part of NBD (amino acids 257–433) partially lost their activity to inhibit Nek2A (Fig. 7A,C). Thus, the region with amino acids 257–433 in Cep85 is responsible for suppressing Nek2A kinase activity.

To examine whether this region is able to bind to Nek2A, we subsequently generated Myc-tagged truncated mutant constructs of Cep85 (Fig. 7D) and carried out co-immunoprecipitation assays with HA–Nek2A. Comparing to WT, we observed that those mutants containing the intact region comprising amino acids 257–433, including M12, M15, M20 and M21, largely preserved their binding affinity to Nek2A (Fig. 7E). Those mutants containing a partial region of amino acids 257–433, such as M19 and M22, greatly lost their binding capacity to Nek2A (Fig. 7E). Remarkably, the mutant containing amino acids 257–433 alone fully retained the binding affinity, which was comparable to WT (Fig. 7E). In contrast, the internal deletion mutant M23, possessing all regions other than amino acids 257–433, completely lost its capability to bind to Nek2A (Fig. 7E). These results suggest that Cep85 binds to Nek2A through its internal region at amino acids 257–433 and inhibits Nek2A kinase activity. Thus, we defined the internal region with at amino acids 257–433 in Cep85 as a Nek2A-binding domain (NBD).

Both the Nek2A binding and centrosomal localization domains are required for Cep85 function in cells

Our *in vitro* kinase assay has clearly demonstrated that the NBD, located at amino acids 257–433, in Cep85 is sufficient to suppress Nek2 kinase activity and the centrosome localization domain at amino acids 434–476 together with the other regions are not essential for its inhibitory activity towards Nek2A (Fig. 7). We thus decided to examine whether the NBD region in Cep85 was also fully functional and suppressed centrosome disjunction in cells. Consistently, WT Cep85 when overexpressed could efficiently suppress centrosome disjunction (Fig. 8A–F); those truncated mutants not containing the NBD, including M1, M9 and M10, completely lost their capacity to suppress centrosome disjunction (Fig. 8). However, the mutant M5, which contains the NBD alone and retains the full inhibitory effect on Nek2 kinase activity *in vitro* (Fig. 7C), only partly prevented centrosome disjunction. Compared to those cells expressing WT Cep85, where ∼80% of them display nonseparated centrosome, only ∼40% of M5-expressed cells exhibited nonseparated centrosome (Fig. 8). In addition, the mutant M7, containing the centrosome localization domain and partial NBD, did not demonstrate any significant inhibitory activity (Fig. 8). Strikingly, the mutant M2 with these two domains joined together became fully functional (Fig. 8). The percentage of cells with nonseparated centrosome appeared to be ∼72%, close to that of WT (∼80%) (Fig. 8F). Thus, both the Nek2A-binding and centrosome localization domains are strictly required for Cep85 to efficiently suppress centrosome disjunction in cells.

DISCUSSION

In current study, through affinity purification and mass spectrometry, we isolated and identified Cep85 as a binding partner of Nek2A. Further *in vitro* and *in vivo* studies confirmed the interaction of Cep85 and Nek2A. Moreover, immunofluorescence analysis revealed that endogenous Cep85 and Nek2A colocalize at centrosomes (Fig. 4). Importantly, Cep85 has been shown to localize to the proximal ends of centrioles, where Nek2A also localizes and functions as a kinase to phosphorylate the proteinaceous linker connecting two mother centrioles (Bahe et al., 2005; Fry et al., 1998a; Mardin and Schiebel, 2012). These findings reveal that Cep85 is a bona fide Nek2A-binding partner in cells.

To our surprise, at first glance, transient overexpression of Cep85 in both synchronized and unsynchronized cells did not cause significant defect in cell cycle progression. However, once treated with Eg5 inhibitor STLC, most Cep85-expressing cells arrested at prometaphase displayed centrosome disjunction failure and retained rootletin between two nonseparated centrosomes (Fig. 5). These results are exactly like those observed in cells with Nek2A depletion (Mardin et al., 2010). Similar results have also been shown by other treatments leading to reduction of Nek2A activity, such as inhibiting Plk1 using SB2536, inhibiting Aurora A with VX-680 and depletion of Mst1 and Mst2, or Sav1 (Mardin et al., 2011, 2010). By contrast, Cep85 depletion results in premature centrosome splitting and loss of rootletin at separated centrosomes in interphase (Fig. 6), strikingly reminiscent of Nek2A hyperactivation (Faragher and Fry, 2003; Fry et al., 1998b; Mardin et al., 2011). Importantly, co-overexpression of Cep85 with Nek2A could prevent the loss of rootletin at centrosomes caused by Nek2A overexpression in interphase (Fig. 5L). Thus, the results of the experiments with up- and down-regulation of Cep85 expression strongly suggest that Cep85 plays roles opposite to those of Nek2A in the maintenance of centrosome conjunction by suppressing Nek2A activity. Biochemically, we identified the

Journal of Cell Science (2015) 128, 3290-3303 doi:10.1242/jcs.171637

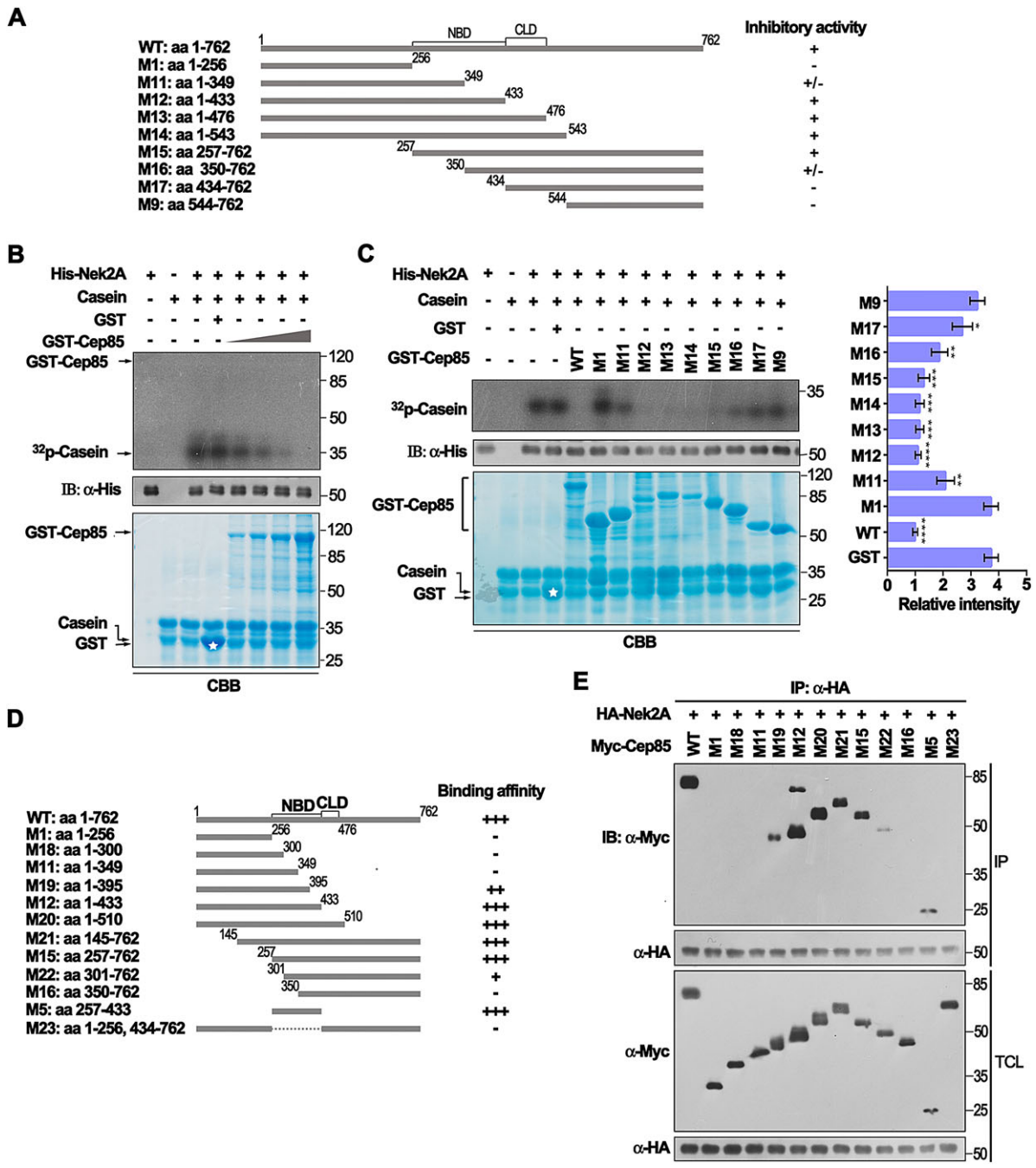

Fig. 7. Cep85 inhibits the kinase activity of Nek2A and the NBD in Cep85 is required for its activity. (A) A schematic of Cep85 and its truncated mutants used in C are shown. The numbers indicate the positions of the first or the last amino acid of individual fragments. +, positive; +/–, partial; –, negative for inhibitory activity against Nek2A. (B) Cep85 inhibits the kinase activity of Nek2A in a dosage-dependent manner. The kinase activity of the purified recombinant His–Nek2A was determined using an *in vitro* kinase assays with β-casein as a substrate. The autoradiography shows [^{32}P]β-casein. Purified recombinant GST–Cep85, GST protein and β-casein were visualized by Coomassie Brilliant Blue (CBB) stain. The asterisk indicates the position of GST protein. Nek2A levels were detected with an anti-His antibody (IB). (C) The NBD, amino acids 257–433 in Cep85, is essential for its inhibitory activity towards Nek2A. CBB stain was used to visualize GST–Cep85 proteins, β-casein and GST protein (marked by an asterisk). The autoradiography shows [^{32}P]β-casein, and Nek2A levels were detected with anti-His antibody. The intensities of autoradiograph bands were quantified by densitometry and normalized to WT. The relative intensity was assessed and is shown on the right panel (mean±s.e.m., n=3). *P<0.05; **P<0.01; ***P<0.001; ****P<0.0001 versus GST. (D) The schematic of Cep85 truncated mutants used in E are shown. The numbers indicate the positions of the first or the last amino acid of individual fragments. +++, highest binding affinity to Nek2A; –, no binding to Nek2A. (E) The NBD, amino acids 257–433 in Cep85, is essential for its binding to Nek2A. Myc–Cep85 and its truncated mutants, overexpressed with HA–Nek2A in HEK293T cells, were immunoprecipitated (IP) and analyzed with western blotting.

region comprising amino acids 257–433 as the Nek2A-binding domain (NBD) in Cep85. Similar to WT Cep85, this domain is sufficient to bind to and inhibit Nek2A kinase activity (Fig. 7). We currently do not know exactly how Cep85 can suppress Nek2A kinase activity after it binds to Nek2A through the NBD. We noticed that Cep85, once co-expressed with Nek2A in HEK293T cells, can be phosphorylated (Fig. 1B), suggesting that Cep85 might be a substrate for Nek2A. However, in our *in vitro* kinase assays, we did

Journal of Cell Science (2015) 128, 3290-3303 doi:10.1242/jcs.171637

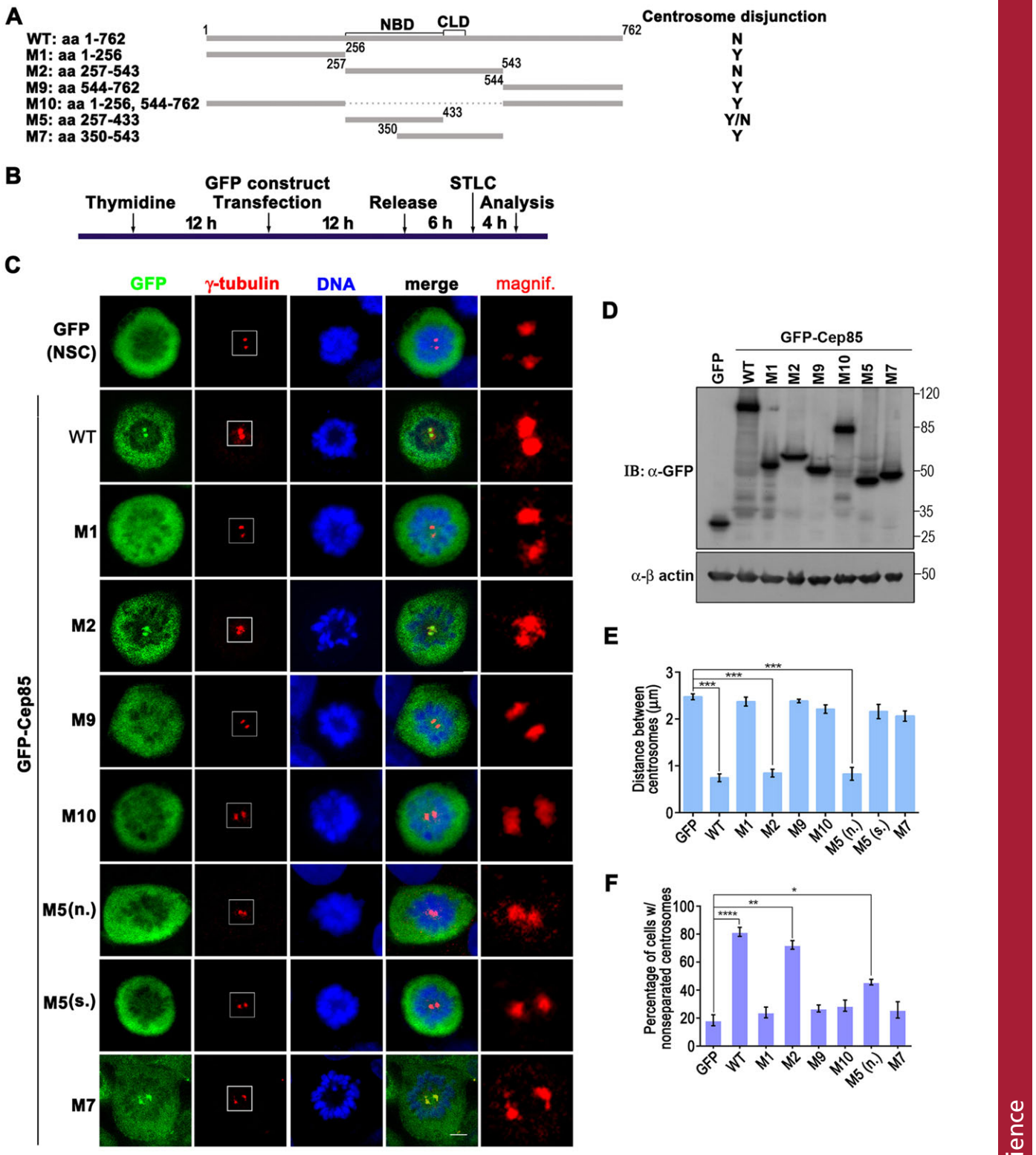

Fig. 8. Both the Nek2-binding and centrosome localization domains in Cep85 are required for its function in cells. (A) A schematic of Cep85 and its truncated mutants used in C–F. The numbers indicate the positions of the first or the last amino acid of individual fragments. Y, yes; Y/N, partial; N, no for whether chromosome disjunction occurs. (B) Schematic outline of experiments in C–F. U2OS cells overexpressing GFP as a control (NSC, non-specific control) or the indicated GFP–Cep85 proteins were enriched at G2 by a single thymidine block and release, and treated with STLC to trap cells in the prometaphase prior to analysis. (C) Cells were fixed and stained for γ-tubulin (red) to indicate centrosomes. The boxed centrosomes are enlarged and are shown on the right. (D) The expression levels of GFP and GFP–Cep85 proteins in U2OS cells are shown by western blotting (IB) with anti-GFP antibody. (E) The distance between two centrosomes for cells in C. Results are from three independent experiments with 20 cells were analyzed for each experiment. Data are mean±s.e.m. ***P<0.001. (F) The histogram indicates the percentage of cell with nonseparated centrosomes. Centrosomes were considered separated when the *distance* between them exceeded 1 μm. Three independent experiments were performed with 20 cells were analyzed for each experiment. Data are mean±s.e.m. *P<0.05; **P<0.01; ****P<0.0001. M5(n.), M5 with nonseparated centrosomes; M5(s.), M5 with separated centrosomes.

Journal of Cell Science (2015) 128, 3290-3303 doi:10.1242/jcs.171637

not detect any incorporation of ^{32}P into a GST–Cep85 protein (Fig. 7B), indicating that Cep85 might not be a substrate for Nek2A. Nevertheless, we found that Cep85 binds to the C-terminus of Nek2A outside of the kinase domain (Fig. 1), which has also been reported to be a pericentrin-binding domain. Whether this binding would cause any structural changes in Nek2A, as has been proposed for pericentrin (Matsuo et al., 2010), is certainly an interesting question and needs for further investigation. Interestingly, the NBD domain alone is not sufficient to efficiently prevent centrosome disjunction in cells, and an additional sequence carrying the centrosome localization domain (CLD) is also required for NBD to fully restore its activity (Fig. 8). Therefore, our data suggest a mode of Cep85 action in which it forms a granule meshwork enveloping the proximal ends of centrioles through its centrosome localization domain, where it interacts with Nek2A through its NBD, suppressing the kinase activity of Nek2A, thereby preventing centrosome splitting in interphase.

Nek2A has been shown to be the major kinase responsible for the phosphorylation and dissociation of the centrosomal linker proteins (Mardin and Schiebel, 2012). Its expression levels and kinase activity remain high in S to G2 phase (Hayes et al., 2006). Meanwhile, overexpression of Nek2A induces premature centrosome disjunction (Faragher and Fry, 2003; Fry et al., 1998b). Therefore, to ensure that the centrosome acts as a single MTOC in interphase, Nek2A kinase activity at centrosomes must be subject to strict control. Multiple levels of regulation have been reported to modulate Nek2A, including its expression, localization, and interaction with inhibitory proteins, like HEF1, pericentrin and PP1 (Fry, 2002; Mardin and Schiebel, 2012). For PP1, it has been demonstrated that PP1γ indirectly antagonizes Nek2A activity by dephosphorylating linker proteins rather than Nek2A *in vivo* (Mardin et al., 2011). Considering that the expression levels and activity of Nek2A are rather high throughout the S and G2 phase of cell cycle, this indirect suppression of Nek2A by PP1γ is certainly necessary but might be inefficient and uneconomic. In conjunction with the action of PP1γ, our model of Cep85 action provides a fairly efficient way to ensure that the two centrosomes will not be separated precociously. We propose that as Nek2A dynamically accumulates to the proximal ends of centrioles where Cep85 localizes, Cep85 binds to and traps it to form a kinase inactive Nek2A–Cep85 complex. The low amount of Nek2A protein that might escape from the trap would bind to and phosphorylate the linker proteins, such as C-Nap1 and rootletin. Immediately, its interacting protein PP1γ will then dephosphorylate them to prevent centrosome splitting in interphase. Although HEF1 and pericentrin might also be involved in restraining Nek2A activity in interphase, it has been suggested that HEF1 could counteract the positive regulation of Nek2A through two Hippo pathway components to prevent the accumulation of Nek2A at centrosomes (Mardin and Schiebel, 2012; Pugacheva and Golemis, 2005). Furthermore, given that neither HEF1 nor pericentrin has been shown to predominantly localize to the proximal ends of centrioles, they might not be heavily involved in the regulation of Nek2A activity there. As both Cep85 and PP1γ interact with Nek2A and reside at centrosomes at the proximal ends of centrioles at the right time, it is likely that our proposed mechanism is crucial for maintaining centrosome integrity in interphase.

In our studies, we have clearly demonstrated that Cep85 can suppress Nek2A activity. We have also found that Cep85 protein exists in all the cell lines we tested but the levels are different in our preliminary studies (Fig. 2). Given that Nek2A activity has been found to be elevated in many human tumors (Cappello et al., 2014; Hayward and Fry, 2006), it will be of great interest to examine the relevance of these two proteins by comparing the levels of Cep85 in primary cell lines with those in related cancer lines, as well as the levels in normal tissues with those in tumor samples, especially samples with high Nek2A activity.

MATERIALS AND METHODS

Plasmids and constructs

Human Cep85 coding sequence (NCBI accession number: NM_022778.3) was amplified from a cDNA library prepared by reverse transcription of total RNA isolated from HEK293T cells and subcloned into the mammalian expression vector pcDNA3.3-HA. This construct was verified by full-length sequencing and further subcloned into pcDNA-Myc, pEGFP-C3 and pGEX-4T-1 vectors. The truncated mutant constructs of Cep85 were prepared either by PCR amplification or subcloning using restriction enzymes with the parental construct pcDNA3.3-HA-Cep85 as a template. Nek2A (NCBI accession number: NM_002497) was cloned from HEK293T by RT-PCR and inserted into pcDNA3.3-Myc and pcDNA3.3-HA vectors. The kinase-dead Nek2A mutant (Nek2A K37R) was created by PCR-based site-directed mutagenesis as described previously (Fry et al., 1995). The truncated mutant Nek2A constructs were generated by PCR amplification. Nek2A was also subcloned into the donor vector pFastBac-HTA (Invitrogen) for expressing recombinant His-tagged Nek2A in insect cells. Centrin 1 was amplified from the HEK293T cDNA library and subcloned into peGFP-N1 for establishment of the centrin1–GFP stable cell line. Primer sequences used for PCR amplification and mutagenesis are available on request. All constructs were confirmed by sequencing.

Cell culture, transfection, primary cilium induction and stable cell line establishment

Mouse fibroblast NIH 3T3, HEK 293T, human cervical cancer HeLa and human osteosarcoma U2OS cell lines were purchased from the ATCC. Cells were grown in high-glucose Dulbecco's modified Eagle's medium (Hyclone) plus 10% fetal bovine serum (Hyclone) and 100 IU/ml penicillin and 100 µg/ml streptomycin at 37°C in a humidified 5% CO_2 incubator. Transient transfection of HEK293T was carried out with the cationic polymer polyethylenimine (PEI) according to the previous report (Boussif et al., 1995). TurboFect reagent (Thermo Scientific) was used to transfect HeLa and U2OS cells according to the manufacturer's instruction. To induce primary cilium formation, the growth medium was replaced with serum-free medium for NIH 3T3 cells for 24 h. To establish U2OS cell lines stably expressing centrin1–GFP, parental U2OS cells were transiently transfected with peGFP-N1-Centrin1 and selected with 50 µg/ml G418 for 2 weeks. Individual clones were picked up, multiplied and analyzed by fluorescence microscopy. Clones with a high signal-to-noise ratio were expanded for further analysis.

Protein expression, immunoprecipitation and western blotting

Recombinant GST fusion Cep85 proteins were expressed in *E. coli* by transforming various pGEX-4T-1-Cep85 constructs into BL21 (DE3) bacteria, induced with 0.25 mM of IPTG, and affinity purified using glutathione–agarose resin (Thermo Scientific). Recombinant His–Nek2A protein was expressed in Sf9 insect cells using pFastBac-HTA-Nek2A as a donor plasmid according to the instruction manual of the Bac-To-Bac Baculovirus Expression System (Invitrogen) and affinity purified with Protino Ni-NTA Agarose (Macherey-Nagel).

For immunoprecipitation and western blotting, briefly, mammalian cells were lyzed in ice-cold cell lysis buffer containing 50 mM Tris-HCl pH 7.4, 150 mM NaCl, 1 mM EDTA and 0.5% NP-40, supplemented with 10 µg/ml pepstatin A, 10 µg/ml leupeptin and 1 mM PMSF. Cleaned cell lysates were incubated with antibodies at 4°C for 2 h prior to incubation with Protein A/G PLUS-Agarose (Santa Cruz Biotechnology) for an extra 2 h. The immunoprecipitates were washed, boiled in SDS sample buffer and resolved by SDS–PAGE. Western blotting was performed using standard protocols and the protein signal was visualized by chemiluminescence using the SuperSignal West Pico system (Thermo Scientific). β-actin was used as a loading control. Antibodies used included: rabbit anti-Cep85 (this study;

1:1000), mouse anti-Nek2A (BD Biosciences; 1:1000), mouse anti-Myc (SC-40, Santa Cruz Biotechnology; 1:1000), mouse anti-FLAG M2 antibody (F1804, Sigma-Aldrich; 1:500), mouse anti-HA (SC-7329, Santa Cruz Biotechnology; 1:1000), mouse anti-β-actin (AC15, Sigma-Aldrich; 1:5000), mouse anti-GST (26H1, Cell Signaling; 1:2000), mouse anti-cyclin B (GNS-1, BD Biosciences; 1:1000), rabbit anti-GFP (Ab290; Abcam; 1:5000) and mouse anti-His_6 (ProteinTech; 1:5000) antibodies.

siRNA

RNA oligonucleotides duplexes were synthesized by Shanghai GenePharma (Shanghai, China) and the sequences were as follows: Cep85, 5′-CCAACAGAACAAGUCCAUUtt-3′; Nek2A, 5′-AAACAUC-GUUCGUUACUAUtt-3′; and negative control siRNA, 5′-UUCUCCGA-ACGUGUCACGUtt-3′. All siRNAs were transfected using ribo*FECT* CP (RiboBio, Guangzhou, China) and cells were analyzed 72 h after transfection.

Cell synchronization

The double thymidine block was carried out as follows: cells were first incubated for 18 h with 2.5 mM thymidine followed by three quick washes with PBS and release in thymidine-free medium for 10 h. They were further incubated with 2.5 mM thymidine for an additional 16 h. Cells were washed three times with PBS, returned to fresh medium and allowed to grow for 2–16 h before harvesting the synchronized cells at different stages of cell cycle for analysis. To enrich cells at a specific stage, a single thymidine block was frequently used in this study. Cells were incubated in culture medium with 2.5 mM thymidine for 18–24 h, washed three times with PBS and then returned to fresh medium for hours. In some cases, 5 μM S-trityl-l-cysteine (STLC) was added to the medium 6 h after release to arrest cells at prometaphase.

Immunofluorescence microscopy

For immunofluorescence, cells were fixed with ice-cold methanol for 5 min, blocked with 5% (v/v) bovine serum albumin (BSA) and 0.05% Triton X-100 in PBS for at least 30 min. Cells were subsequently incubated with primary antibodies with 5% (v/v) BSA and 0.05% Triton X-100 in PBS for 1 h followed by five washes with 0.1% Triton X-100 in PBS for a total of 30 min and another 1 h incubation with secondary antibodies. DNA was stained with DAPI (0.2 μg/ml; Invitrogen). Primary antibodies included rabbit anti-Cep85 (this study; 1:100), Alexa-Fluor-555-conjugated rabbit anti-Cep85 (this study; 1:10), mouse anti-γ-tubulin (T6557, Sigma-Aldrich; 1:2000), mouse anti-Nek2 (BD Biosciences; 1:200), rabbit anti-c-Myc (C-3956, Sigma-Aldrich; 1:400), rabbi anti-HA-tag (H6908, Sigma-Aldrich; 1:500), mouse anti-Sas-6 (SC-81431; 1:200), mouse anti-acetylated tubulin (T6793, Sigma-Aldrich; 1:500), rabbit anti-pericentrin (ab4448, Abcam; 1:3000), goat anti-rootletin (Santa Cruz Biotechnology; 1:500), rabbit anti-C-Nap1 (14498-1-AP, Proteintech, 1:1000). Secondary antibodies included donkey anti-mouse-IgG conjugated to Alexa Fluor 488, anti-rabbit-IgG conjugated to Alexa Fluor 488, anti-mouse-IgG conjugated to Alexa Fluor 555, anti-rabbit-IgG conjugated to Alexa Fluor 555 and anti-goat-IgG conjugated to Alexa Fluor 594 (Invitrogen). Images were acquired using a Zeiss LSM 780 laser-scanning confocal microscope (Carl Zeiss, Germany), or Axio Imager D2 equipped with AxioCam HRM (Carl Zeiss, Germany). Three-dimensional structured illumination microscope (3D-SIM) images were acquired on a DeltaVision OMX V4 microscope (Applied Precision, GE Healthcare, Issaquah, WA) equipped with a ×63, 1.42 NA Olympus objective. Data were reconstructed using API SoftWorx software.

In vitro kinase assays

The *in vitro* Nek2A kinase activity measurement was performed as described previously (Fry et al., 1995). To examine the effects of Cep85 and its derivatives on Nek2A kinase activity, the recombinant Cep85 proteins were expressed and purified from *E. coli* and His–Nek2A was expressed and purified from Sf9 cells. The kinase reaction was carried out by incubating 0.02 mg/ml of His–Nek2A with ∼0.2 mg/ml of the GST-tagged Cep85 WT or truncated mutants in a total volume of 50 μl for 30 min at 30°C. GST protein was also included as a negative control. 0.5 mg/ml β-casein (Sigma-Aldrich, C-4032), as a substrate for Nek2A, was added to the kinase buffer containing 20 mM Tris-HCl pH 7.5, 50 mM KCl, 10 mM $MgCl_2$, 1 mM DTT, 4 μM ATP and 10 μCi [γ-^{32}P]ATP (Amersham). The amount of GST–Cep85 used for the experiment in Fig. 2B was 2 μg, 4 μg, 6 μg and 10 μg in a total volume of 50 μl. The reaction was terminated by adding 50 μl of 2× SDS sample buffer and boiling at 95°C for 10 min. The samples were solved by SDS-PAGE, stained with Coomassie Brilliant Blue (CBB) and subjected to autoradiography. His–Nek2A levels in the samples were visualized by western blotting.

Measurement and statistics

ZEN 2010 software (Carl Zeiss, Germany) was used for measurement. The fluorescent intensity of Nek2A and γ-tubulin at centrosome and the distance of centrosomes were measured according to the methods previously described (Mardin et al., 2010). Statistical significance was determined by unpaired two-tailed Student's *t*-tests. Differences were considered as significant when $P<0.05$.

Acknowledgements

We thank Dr X. Li for kindly providing antibody against diversin and Dr G. Li for assistance with performing the phylogenetic tree analysis.

Competing interests

The authors declare no competing or financial interests.

Author contributions

C.C. and X.Y. conceived and designed the experiments. C.C., L.L. and F.T. performed the experiments and analyzed the data with the help of Y.W., Z.X. and C.Y. C.C. and X.Y. interpreted the data and wrote the manuscript.

Funding

This work was supported by the National Natural Science Foundation of China [grant numbers 31471260, 31171286 to X.Y.]; and Project 111 sponsored by the State Bureau of Foreign Experts and Ministry of Education [grant number B06016]. Deposited in PMC for immediate release.

Supplementary material

Supplementary material available online at
http://jcs.biologists.org/lookup/suppl/doi:10.1242/jcs.171637/-/DC1

References

Bahe, S., Stierhof, Y.-D., Wilkinson, C. J., Leiss, F. and Nigg, E. A. (2005). Rootletin forms centriole-associated filaments and functions in centrosome cohesion. *J. Cell Biol.* **171**, 27-33.

Bettencourt-Dias, M. and Glover, D. M. (2007). Centrosome biogenesis and function: centrosomics brings new understanding. *Nat. Rev. Mol. Cell Biol.* **8**, 451-463.

Bornens, M. (2002). Centrosome composition and microtubule anchoring mechanisms. *Curr. Opin. Cell Biol.* **14**, 25-34.

Bornens, M., Paintrand, M., Berges, J., Marty, M.-C. and Karsenti, E. (1987). Structural and chemical characterization of isolated centrosomes. *Cell. Motil. Cytoskeleton* **8**, 238-249.

Boussif, O., Lezoualc'h, F., Zanta, M. A., Mergny, M. D., Scherman, D., Demeneix, B. and Behr, J. P. (1995). A versatile vector for gene and oligonucleotide transfer into cells in culture and in vivo: polyethylenimine. *Proc. Natl. Acad. Sci. USA* **92**, 7297-7301.

Cappello, P., Blaser, H., Gorrini, C., Lin, D. C. C., Elia, A. J., Wakeham, A., Haider, S., Boutros, P. C., Mason, J. M., Miller, N. A. et al. (2014). Role of Nek2 on centrosome duplication and aneuploidy in breast cancer cells. *Oncogene* **33**, 2375-2384.

Eto, M., Elliott, E., Prickett, T. D. and Brautigan, D. L. (2002). Inhibitor-2 regulates protein phosphatase-1 complexed with NimA-related kinase to induce centrosome separation. *J. Biol. Chem.* **277**, 44013-44020.

Faragher, A. J. and Fry, A. M. (2003). Nek2A kinase stimulates centrosome disjunction and is required for formation of bipolar mitotic spindles. *Mol. Biol. Cell* **14**, 2876-2889.

Fry, A. M. (2002). The Nek2 protein kinase: a novel regulator of centrosome structure. *Oncogene* **21**, 6184-6194.

Fry, A. M., Schultz, S. J., Bartek, J. and Nigg, E. A. (1995). Substrate specificity and cell cycle regulation of the Nek2 protein kinase, a potential human homolog of the mitotic regulator NIMA of Aspergillus nidulans. *J. Biol. Chem.* **270**, 12899-12905.

Fry, A. M., Mayor, T., Meraldi, P., Stierhof, Y.-D., Tanaka, K. and Nigg, E. A. (1998a). C-Nap1, a novel centrosomal coiled-coil protein and candidate substrate of the cell cycle-regulated protein kinase Nek2. *J. Cell. Biol.* **141**, 1563-1574.

Fry, A. M., Meraldi, P. and Nigg, E. A. (1998b). A centrosomal function for the human Nek2 protein kinase, a member of the NIMA family of cell cycle regulators. *EMBO J.* **17**, 470-481.
Glover, D. M., Hagan, I. M. and Tavares, A. A. M. (1998). Polo-like kinases: a team that plays throughout mitosis. *Genes Dev.* **12**, 3777-3787.
Golsteyn, R. M., Mundt, K. E., Fry, A. M. and Nigg, E. A. (1995). Cell cycle regulation of the activity and subcellular localization of Plk1, a human protein kinase implicated in mitotic spindle function. *J. Cell Biol.* **129**, 1617-1628.
Hames, R. S. and Fry, A. M. (2002). Alternative splice variants of the human centrosome kinase Nek2 exhibit distinct patterns of expression in mitosis. *Biochem. J.* **361**, 77-85.
Hames, R. S., Wattam, S. L., Yamano, H., Bacchieri, R. and Fry, A. M. (2001). APC/C-mediated destruction of the centrosomal kinase Nek2A occurs in early mitosis and depends upon a cyclin A-type D-box. *EMBO J.* **20**, 7117-7127.
Hayes, M. J., Kimata, Y., Wattam, S. L., Lindon, C., Mao, G., Yamano, H. and Fry, A. M. (2006). Early mitotic degradation of Nek2A depends on Cdc20-independent interaction with the APC/C. *Nat. Cell Biol.* **8**, 607-614.
Hayward, D. G. and Fry, A. M. (2006). Nek2 kinase in chromosome instability and cancer. *Cancer Lett.* **237**, 155-166.
He, R., Huang, N., Bao, Y., Zhou, H., Teng, J. and Chen, J. (2013). LRRC45 is a centrosome linker component required for centrosome cohesion. *Cell Rep.* **4**, 1100-1107.
Helps, N. R., Luo, X., Barker, H. M. and Cohen, P. T. W. (2000). NIMA-related kinase 2 (Nek2), a cell-cycle-regulated protein kinase localized to centrosomes, is complexed to protein phosphatase 1. *Biochem. J.* **349**, 509-518.
Jakobsen, L., Vanselow, K., Skogs, M., Toyoda, Y., Lundberg, E., Poser, I., Falkenby, L. G., Bennetzen, M., Westendorf, J., Nigg, E. A. et al. (2011). Novel asymmetrically localizing components of human centrosomes identified by complementary proteomics methods. *EMBO J.* **30**, 1520-1535.
Leidel, S., Delattre, M., Cerutti, L., Baumer, K. and Gönczy, P. (2005). SAS-6 defines a protein family required for centrosome duplication in C. elegans and in human cells. *Nat. Cell Biol.* **7**, 115-125.
Mardin, B. R. and Schiebel, E. (2012). Breaking the ties that bind: new advances in centrosome biology. *J. Cell Biol.* **197**, 11-18.
Mardin, B. R., Lange, C., Baxter, J. E., Hardy, T., Scholz, S. R., Fry, A. M. and Schiebel, E. (2010). Components of the Hippo pathway cooperate with Nek2 kinase to regulate centrosome disjunction. *Nat. Cell Biol.* **12**, 1166-1176.
Mardin, B. R., Agircan, F. G., Lange, C. and Schiebel, E. (2011). Plk1 controls the Nek2A-PP1gamma antagonism in centrosome disjunction. *Curr. Biol.* **21**, 1145-1151.
Matsuo, K., Nishimura, T., Hayakawa, A., Ono, Y. and Takahashi, M. (2010). Involvement of a centrosomal protein kendrin in the maintenance of centrosome cohesion by modulating Nek2A kinase activity. *Biochem. Biophys. Res. Commun.* **398**, 217-223.
Meraldi, P. and Nigg, E. A. (2001). Centrosome cohesion is regulated by a balance of kinase and phosphatase activities. *J. Cell Sci.* **114**, 3749-3757.
Mi, J., Guo, C., Brautigan, D. L. and Larner, J. M. (2007). Protein phosphatase-1alpha regulates centrosome splitting through Nek2. *Cancer Res.* **67**, 1082-1089.
Nam, H.-J. and van Deursen, J. M. (2014). Cyclin B2 and p53 control proper timing of centrosome separation. *Nat. Cell Biol.* **16**, 538-549.
Nigg, E. A. (2006). Cell biology: a licence for duplication. *Nature* **442**, 874-875.
Nigg, E. A. and Raff, J. W. (2009). Centrioles, centrosomes, and cilia in health and disease. *Cell* **139**, 663-678.
O'Regan, L., Blot, J. and Fry, A. M. (2007). Mitotic regulation by NIMA-related kinases. *Cell Division* **2**, 25.
Pugacheva, E. N. and Golemis, E. A. (2005). The focal adhesion scaffolding protein HEF1 regulates activation of the Aurora-A and Nek2 kinases at the centrosome. *Nat. Cell Biol.* **7**, 937-946.
Spalluto, C., Wilson, D. I. and Hearn, T. (2012). Nek2 localises to the distal portion of the mother centriole/basal body and is required for timely cilium disassembly at the G2/M transition. *Eur. J. Cell Biol.* **91**, 675-686.
Tsou, M.-F. and Stearns, T. (2006). Mechanism limiting centrosome duplication to once per cell cycle. *Nature* **442**, 947-951.
Zhou, H., Kuang, J., Zhong, L., Kuo, W.-L., Gray, J., Sahin, A., Brinkley, B. and Sen, S. (1998). Tumour amplified kinase STK15/BTAK induces centrosome amplification, aneuploidy and transformation. *Nat. Genet.* **20**, 189-193.